

.. ... 62.82949

Copy 20
RM SL54I29

N65-88104

FACILITY FORM 602

ACCESSION NUMBER

(PAGES)

(NASA CR OR TMX OR AD NUMBER)

(THRU)

(CODE)

(CATEGORY)

NACA

RESEARCH MEMORANDUM

for the

Bureau of Aeronautics, Department of the Navy

WIND-TUNNEL INVESTIGATION AT LOW SPEED OF THE ROLLING
STABILITY DERIVATIVES OF A 1/10-SCALE MODEL
OF THE DOUGLAS A4D-1 AIRPLANE

TED NO. NACA DE 389

By Walter D. Wolhart and H. S. Fletcher

Langley Aeronautical Laboratory
Langley Field, Va.

Declassified by authority of NASA
Classification Change Notices No. 7-10
Dated 11/12/61

Authority: Memo Geo. Drobka NASA HQ.
Code ATSS-A Dtd. 3-12-64 Subj: Change
in Security Classification Marking

NATIONAL ADVISORY COMMITTEE
FOR AERONAUTICS

WASHINGTON

OCT 7 1954

NACA RM SL54I29

X-2484

DECLASSIFIED

NATIONAL ADVISORY COMMITTEE FOR AERONAUTICS

RESEARCH MEMORANDUM

for the

Bureau of Aeronautics, Department of the Navy

WIND-TUNNEL INVESTIGATION AT LOW SPEED OF THE ROLLING
STABILITY DERIVATIVES OF A 1/10-SCALE MODEL
OF THE DOUGLAS A4D-1 AIRPLANE

TED NO. NACA DE 389

By Walter D. Wolhart and H. S. Fletcher

DECLASSIFIED - EFFECTIVE 1-25-64
Authority: Memo Geo. Drobka NASA HQ.
Code ATSS-A Dtd. 3-12-64 Subj: Change
in Security Classification Markings

SUMMARY

An experimental investigation has been made in the Langley stability tunnel to determine the low-speed rolling stability derivatives of a 1/10-scale model of the Douglas A4D-1 airplane. The model was tested in clean and landing configurations with horizontal and vertical tails on and off. The effect of removing the horizontal tail was determined for one of the clean configurations. The effects of external wing stores were determined for one complete clean configuration, one complete landing configuration, and one landing configuration with horizontal and vertical tails off. Also included in the investigation were the effects of slats and flaps on the derivatives of the wing alone. These data are presented without analysis in order to expedite distribution.

INTRODUCTION

An important design objective in the development of any airplane is the attainment of acceptable dynamic-flight characteristics. Previous experience has indicated that reliable prediction of the dynamic-flight characteristics for a wide angle-of-attack range requires more accurate estimates of the various aerodynamic parameters than is possible with the use of available procedures. (See refs. 1 and 2, for example.)

The purpose of the present investigation was to determine the rolling stability derivatives of a 1/10-scale model of the Douglas A4D-1 airplane over a wide angle-of-attack range from a series of low-speed tests in the Langley stability tunnel. These tests were made at

DECLASSIFIED

the request of the Bureau of Aeronautics, Department of the Navy, to aid in the development of the Douglas A4D-1 airplane. The results of previous investigations to determine the static lateral and longitudinal stability derivatives and the yawing stability derivatives of the same model are given in references 3 and 4, respectively.

SYMBOLS

The data presented herein are in the form of standard NACA coefficients of forces and moments which are referred to the stability system of axes with the origin at the center of gravity. The positive direction of forces, moments, and angular displacements is shown in figure 1. The coefficients and symbols are defined as follows:

L	lift, lb
D	drag, lb
Y	side force, lb
M	pitching moments, ft-lb
L'	rolling moment, ft-lb
N	yawing moment, ft-lb
b	span, ft
S	area, sq ft
c	chord, measured parallel to plane of symmetry, ft
\bar{c}	mean aerodynamic chord, $\frac{2}{S} \int_0^{b/2} c^2 dy$
y	spanwise distance from and perpendicular to plane of symmetry, ft
q	free-stream dynamic pressure, $\rho V^2/2$, lb/sq ft
V	free-stream velocity, ft/sec
ρ	mass density of air, slugs/cu ft
α	angle of attack of fuselage reference line, deg

[REDACTED]

γ	flight-path angle, deg
ϕ	angle of roll, radians
i_t	angle of incidence of horizontal tail with respect to fuselage reference line, deg
δ_f	flap deflection, deg
β	angle of sideslip, deg
ψ	angle of yaw, deg
C_Y	lateral-force coefficient, Y/qS_w
C_l	rolling-moment coefficient, $L'/qS_w b_w$
C_n	yawing-moment coefficient, $N/qS_w b_w$
$pb/2V$	rolling-angular-velocity parameter, radians
p	rolling-angular velocity, $d\phi/dt$, radians/sec

$$C_{Y_p} = \frac{\partial C_Y}{\partial \frac{pb}{2V}}$$

$$C_{l_p} = \frac{\partial C_l}{\partial \frac{pb}{2V}}$$

$$C_{n_p} = \frac{\partial C_n}{\partial \frac{pb}{2V}}$$

ΔC_{Y_p} , ΔC_{l_p} , and ΔC_{n_p} tare increments due to support strut (to be subtracted from basic data)

Subscripts:

w	wing
s	wing slats, fully opened
f	split flaps, deflected 50°

c closed landing-gear fairings

For convenience, the model components are denoted by the following symbols:

W wing (when used with subscript s and f denotes slats open and flaps deflected, respectively)

F ducted fuselage (including canopy)

V vertical tail

G landing gear down (when used with subscript c denotes landing gear up and closed landing-gear fairings)

E two pylon-mounted external stores

H horizontal tail

APPARATUS AND MODELS

The tests of the present investigation were made in the 6-foot-diameter rolling-flow test section of the Langley stability tunnel in which rolling flight is simulated by rolling the airstream about a stationary model (ref. 5). Forces and moments on the model were obtained with the model mounted on a single strut support which was in turn fastened to a conventional six-component balance system.

The model used in this investigation was a 1/10-scale model of the Douglas A4D-1 airplane. Pertinent geometric characteristics of the model are given in figure 2 and table I. Photographs of two of the configurations tested are presented in figure 3. The wing, ducted fuselage, tail surfaces, and external wing stores were constructed primarily of laminated mahogany, although the wing and tail surfaces were built up from a 1/4-inch-thick aluminum-alloy core which provided additional stiffness and metal trailing edges. The plain split flaps and landing-gear doors were made from 1/16-inch-thick aluminum sheet and the landing struts were made from brass tubing. The wing leading-edge slats were cast from brass and simulated either a fully opened or fully closed slat position.

TESTS

All the tests were made at a dynamic pressure of 24.9 pounds per square foot which corresponds to a Mach number of about 0.13 and a Reynolds number of 0.99×10^6 based on the wing mean aerodynamic chord of 1.08 feet. The angle-of-attack range for all tests was from approximately -4° to 28° . Tests were made at values of $pb/2V$ of -0.064, -0.042, -0.024, 0, 0.007, 0.029, and 0.056. The various model configurations investigated are shown in table II.

CORRECTIONS

Approximate corrections for jet-boundary effects were applied to the angle of attack by the methods of reference 6. Blockage corrections were determined and applied to the dynamic pressure by the methods of reference 7. These data are not corrected for the effects of the support strut since these effects were determined for only one complete clean and one complete landing configuration. The tares for these two configurations are presented and, if applied, are to be subtracted from the basic data.

PRESENTATION OF RESULTS

The results of this investigation are presented in figures 4 to 8. For convenience in locating desired information, a summary of the configurations investigated as well as the figures that give data for these configurations is given in table III. These data are presented without analysis in order to expedite distribution.

Langley Aeronautical Laboratory,
National Advisory Committee for Aeronautics,
Langley Field, Va., September 17, 1954.

Walter D. Wolhart
Walter D. Wolhart

Aeronautical Research Scientist

H. S. Fletcher
H. S. Fletcher

Aeronautical Research Scientist

Approved:

Charles H. Zimmerman

for Thomas A. Harris
Chief of Stability Research Division

ecc

[REDACTED]

REFERENCES

1. Jaquet, Byron M., and Fletcher, H. S.: Lateral Oscillatory Characteristics of the Republic F-91 Airplane Calculated by Using Low-Speed Experimental Static and Rotary Derivatives. NACA RM L53G01, 1953.
2. Campbell, John P., and McKinney, Marion O.: Summary of Methods for Calculating Dynamic Lateral Stability and Response and for Estimating Lateral Stability Derivatives. NACA Rep. 1098, 1952. (Supersedes NACA TN 2409.)
3. Wolhart, Walter D., and Fletcher, H. S.: Wind-Tunnel Investigation at Low Speed of the Static Lateral and Longitudinal Stability Characteristics of a 1/10-Scale Model of the Douglas A4D-1 Airplane - TED No. NACA DE 389. NACA RM SL54H13, Bur. Aero., 1954.
4. Wolhart, Walter D., and Fletcher, H. S.: Wind-Tunnel Investigation at Low Speed of the Yawing Stability Derivatives of a 1/10-Scale Model of the Douglas A4D-1 Airplane - TED No. NACA DE 389. NACA RM SL54I07, Bur. Aero., 1954.
5. MacLachlan, Robert, and Letko, William: Correlation of Two Experimental Methods of Determining the Rolling Characteristics of Unswept Wings. NACA TN 1309, 1947.
6. Silverstein, Abe, and White, James A.: Wind-Tunnel Interference With Particular Reference to Off-Center Positions of the Wing and to the Downwash at the Tail. NACA Rep. 547, 1936.
7. Herriot, John G.: Blockage Corrections for Three-Dimensional-Flow Closed-Throat Wind Tunnels, With Consideration of the Effect of Compressibility. NACA Rep. 995, 1950. (Supersedes NACA RM A7B28.)

TABLE I.- GEOMETRIC CHARACTERISTICS OF 1/10-SCALE MODEL OF
THE DOUGLAS A4D-1 AIRPLANE

Wing:	
Aspect ratio	2.91
Taper ratio	0.226
Quarter-chord sweep angle, deg	33.21
Dihedral angle (trailing edge), deg	2.67
Geometric twist, deg	0
Incidence at root chord (parallel to fuselage reference line), deg	0
Airfoil section (parallel to fuselage reference line):	
Root	NACA 0008 (mod.)
Tip	NACA 0005 (mod.)
Chord (parallel to fuselage reference line):	
Root, ft	1.550
Tip, ft	0.350
Area, sq ft	2.600
Span, ft	2.750
Mean aerodynamic chord, ft	1.080
Horizontal tail:	
Aspect ratio	2.80
Taper ratio	0.225
Quarter-chord sweep angle, deg	34.37
Dihedral angle, deg	0
Airfoil section (parallel to fuselage reference line):	
Root	NACA 0007 (mod.)
Tip	NACA 0004 (mod.)
Chord (parallel to fuselage reference line):	
Root, ft	0.667
Tip, ft	0.150
Area, sq ft	0.459
Span, ft	1.113
Mean aerodynamic chord, ft	0.466
Tail length, distance from c.g. to $\bar{c}/4$ of tail, ft	1.607
Vertical tail:	
Aspect ratio	1.24
Taper ratio	0.195
Quarter-chord sweep angle, deg	42.00
Airfoil section (parallel to fuselage reference line):	
Root	NACA 0007 (mod.)
Tip	NACA 0004 (mod.)
Chord (parallel to fuselage reference line):	
Root (measured 1.96 inches above fuselage reference line), ft	1.069
Tip, ft	0.208
Area, sq ft	0.500
Span, ft	0.786
Mean aerodynamic chord, ft	0.738
Tail length, distance from c.g. to $\bar{c}/4$ of tail, ft	1.420
Fuselage:	
Maximum width, ft	0.533
Maximum depth, ft	0.500
Length, ft	3.703
Cross-sectional area of duct:	
Inlet (both sides), sq ft	0.0343
Exit, sq ft	0.0179
Lift-increasing devices -	
Wing flaps:	
Type	Split
Maximum deflection, deg	50.00
Actual span (one side), ft	0.592
Chord (parallel to fuselage reference line), ft	0.208
Wing leading-edge slats:	
Slat rotation about hinge line for fully opened position, deg	24.00
Actual span (perpendicular to fuselage reference line) (one side), ft	0.750
Chord (parallel to fuselage reference line):	
Root, ft	0.181
Tip, ft	0.087

0371224030

TABLE II.- CONFIGURATIONS INVESTIGATED

Clean configuration					
Components	Landing gear	Slats	δ_f , deg	i_t , deg	Stores
WFG _C VH	Up	Closed	0	0	Off
WFG _C VHE	Up	Closed	0	0	On
W _S FG _C VH	Up	Open	0	-4	Off
WFG _C V	Up	Closed	0	---	Off
WFG _C	Up	Closed	0	---	Off
W _S FG _C	Up	Open	0	---	Off
W	----	Closed	0	---	---
W _S	----	Open	0	---	---
Landing configuration					
W _f FGVH	Down	Closed	50	-12	Off
W _{sf} FGVH	Down	Open	50	-12	Off
W _{sf} FGVHE	Down	Open	50	-12	On
W _f FG	Down	Closed	50	---	Off
W _{sf} FG	Down	Open	50	---	Off
W _{sf} FGE	Down	Open	50	---	On
W _f	----	Closed	50	---	---
W _{sf}	----	Open	50	---	---

TABLE III.- SUMMARY OF CONFIGURATIONS TESTED AND DATA PRESENTED

Model configuration	Data presented	Figure
WFG _C VH, $i_t = 0^\circ$ WFG _C V W _S FG _C VH, $i_t = -4^\circ$ W _F FGVH, $i_t = -12^\circ$ W _{SF} FGVH, $i_t = -12^\circ$	Effect of high lift devices on complete configurations. C_{Y_p} , C_{n_p} , and C_{l_p} plotted against α .	4
WFG _C VHE, $i_t = 0^\circ$ W _{SF} FGVHE, $i_t = -12^\circ$ W _{SF} FGE	Effect of wing stores on a complete clean configuration, a complete landing configuration, and a landing configuration with the tails off. C_{Y_p} , C_{n_p} , and C_{l_p} plotted against α .	5
WFG _C W _S FG _C W _F FG W _{SF} FG	Effect of high lift devices on tailless configurations. C_{Y_p} , C_{n_p} , and C_{l_p} plotted against α .	6
W W _S W _F W _{SF}	Effect of high lift devices on wing alone. C_{Y_p} , C_{n_p} , and C_{l_p} plotted against α .	7
WFG _C VH, $i_t = 0^\circ$ W _{SF} FGVH, $i_t = -12^\circ$	Tare increments due to the support strut for a complete clean and a complete landing configuration. ΔC_{Y_p} , ΔC_{n_p} , and ΔC_{l_p} plotted against α .	8

037129 130

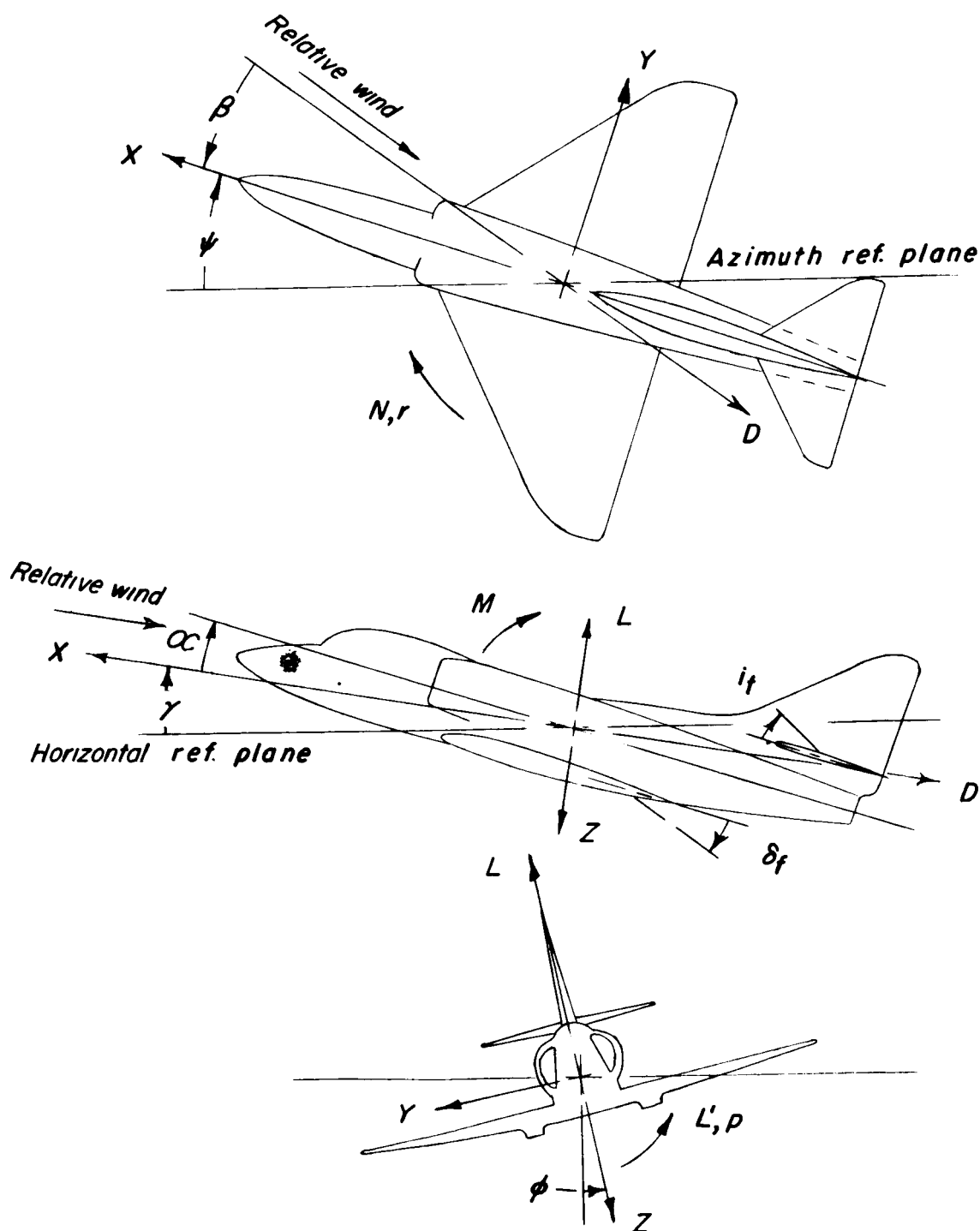


Figure 1.- Stability system of axes. Arrows indicate positive direction of forces, moments, angular displacements, and angular velocities.

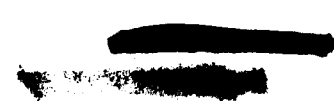
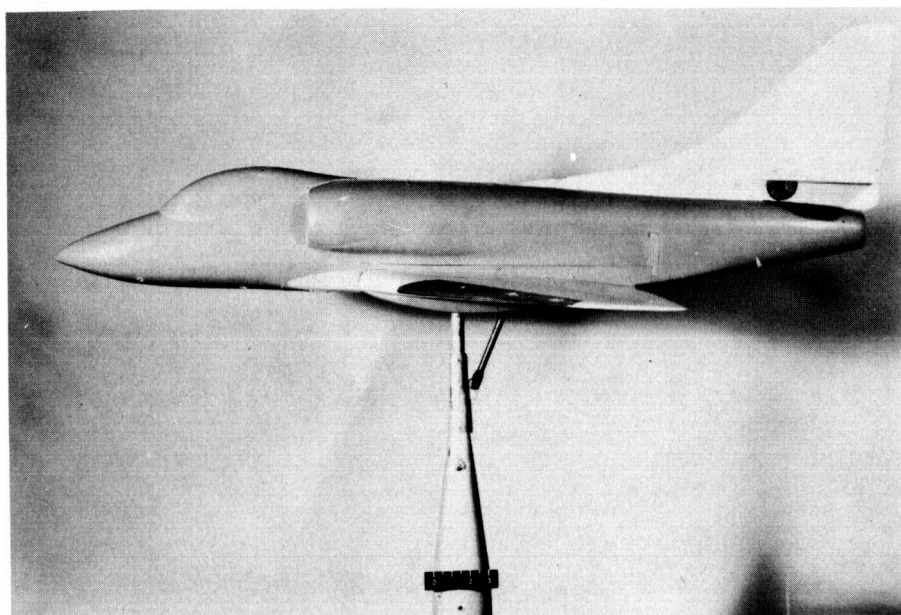
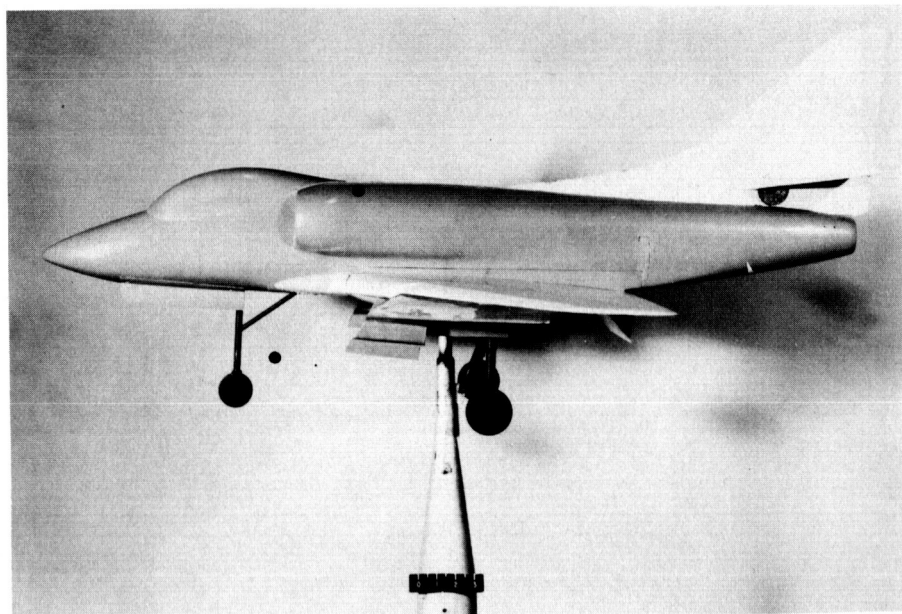


Figure 2.- Geometric characteristics of 1/10-scale model of the Douglas A4D-1 airplane. All dimensions are in inches.



L-84638

(a) Side view of complete clean configuration; $WFG_{c}VH$, $i_t = 0^\circ$.



L-84639

(b) Side view of complete landing configuration; $W_{sf}FGVH$, $i_t = -12^\circ$.

Figure 3.- Photographs of two of the configurations tested.

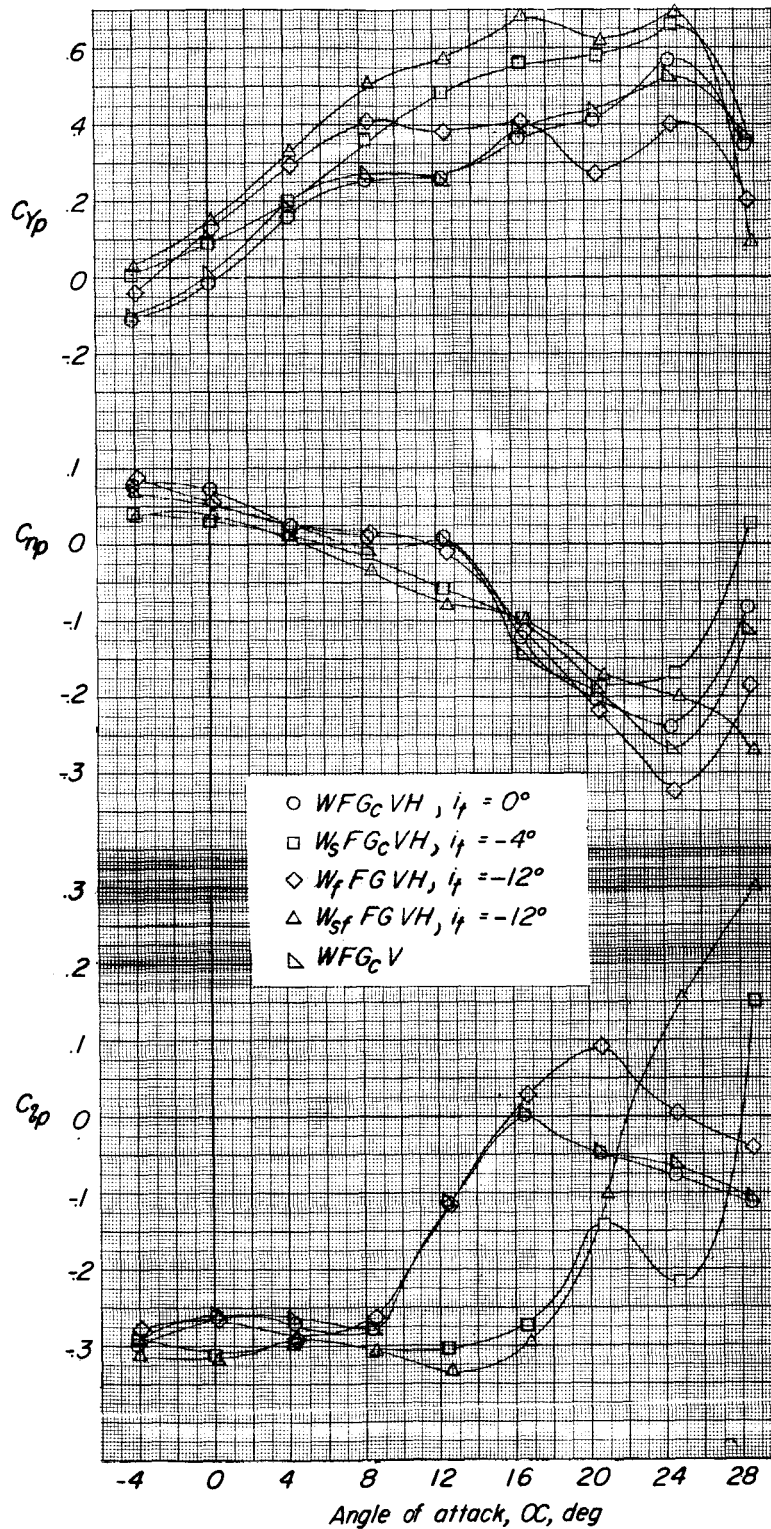


Figure 4.- Effect of horizontal tail and high lift devices on the rolling stability derivatives of the complete model.

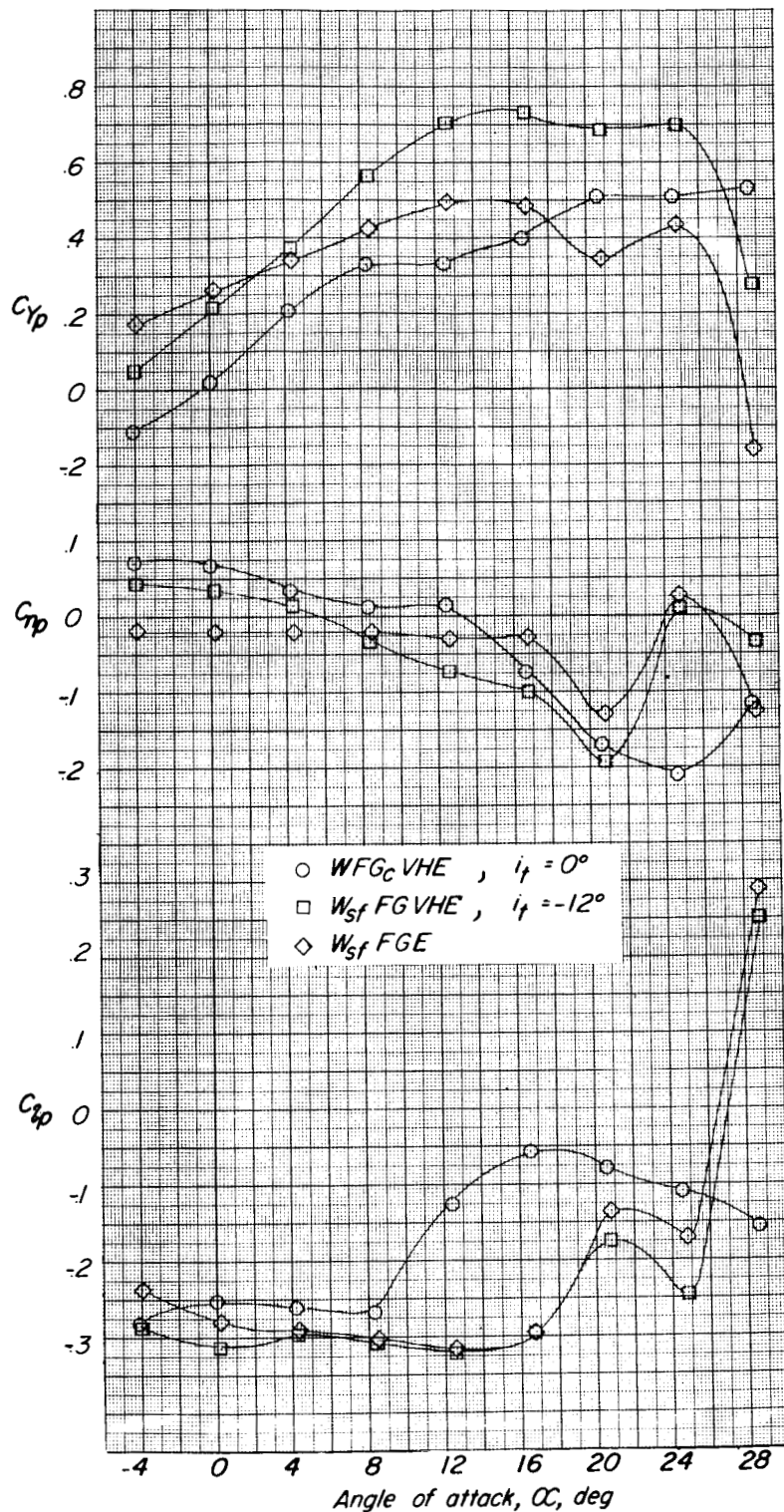


Figure 5.- Effect of wing stores on the rolling stability derivatives of a complete clean configuration, a complete landing configuration, and a landing configuration with the tails off.

DECLASSIFIED

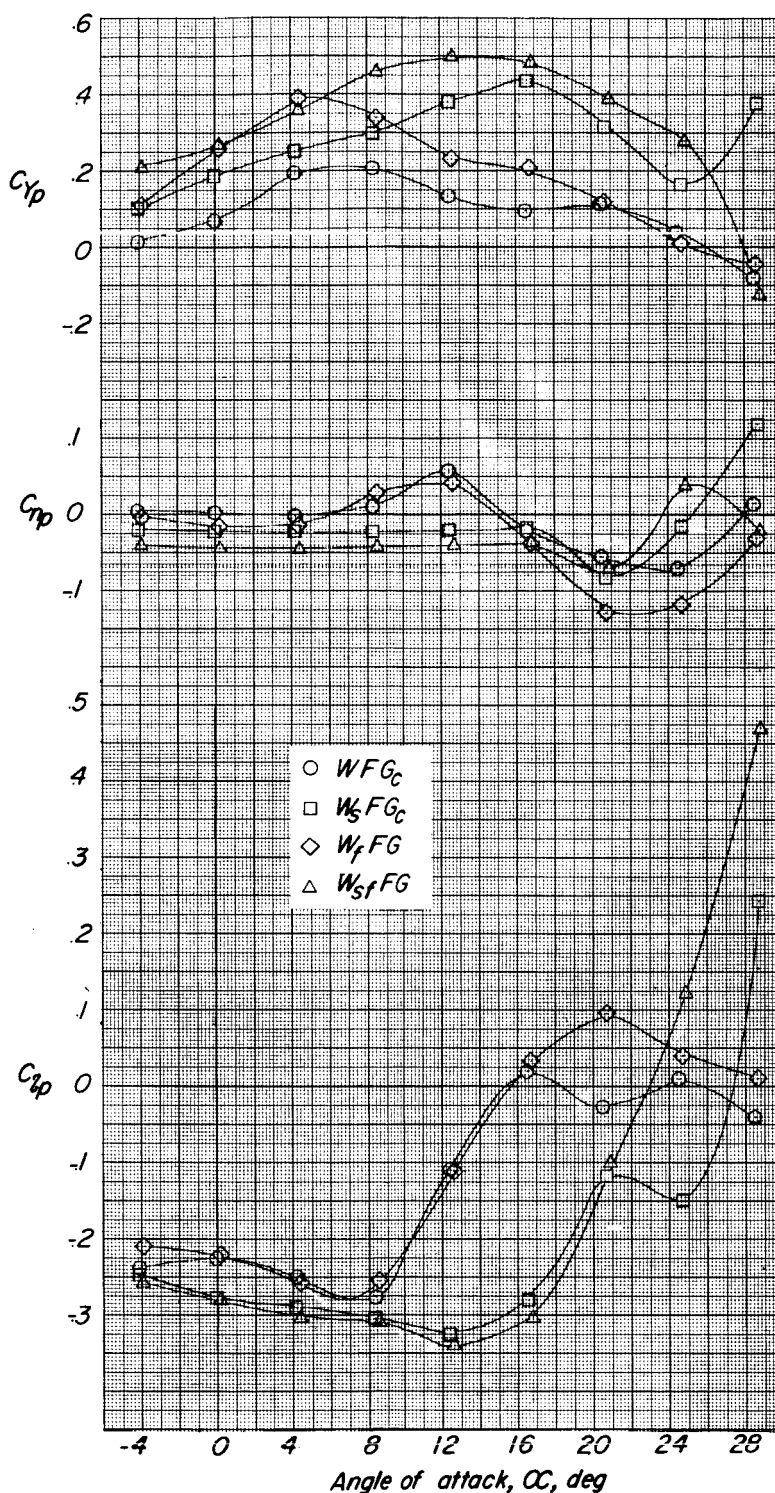


Figure 6.- Effect of high lift devices on the rolling stability derivatives of configurations with horizontal and vertical tails off.

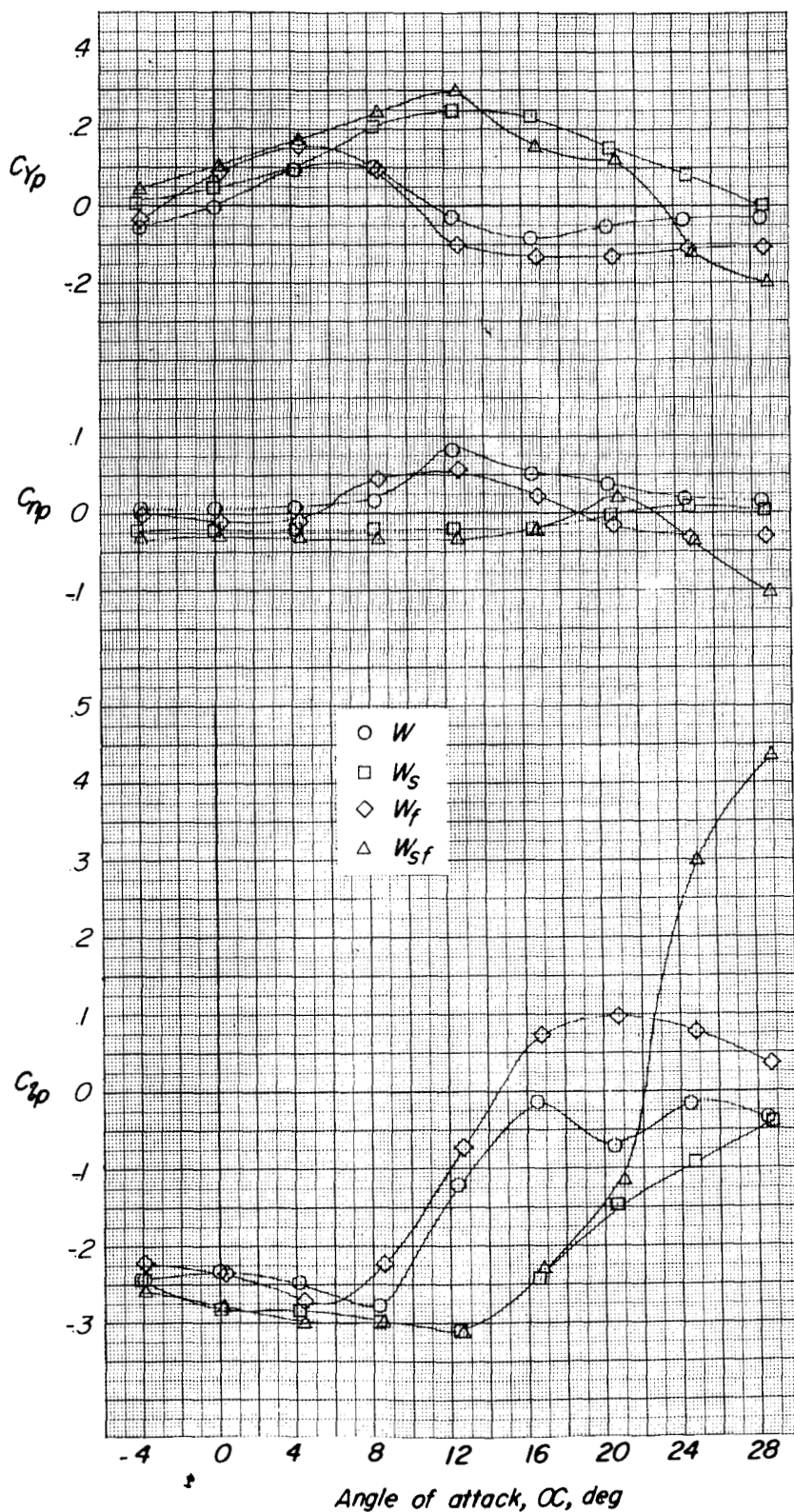


Figure 7.- Effect of high lift devices on the rolling stability derivatives of the wing alone.

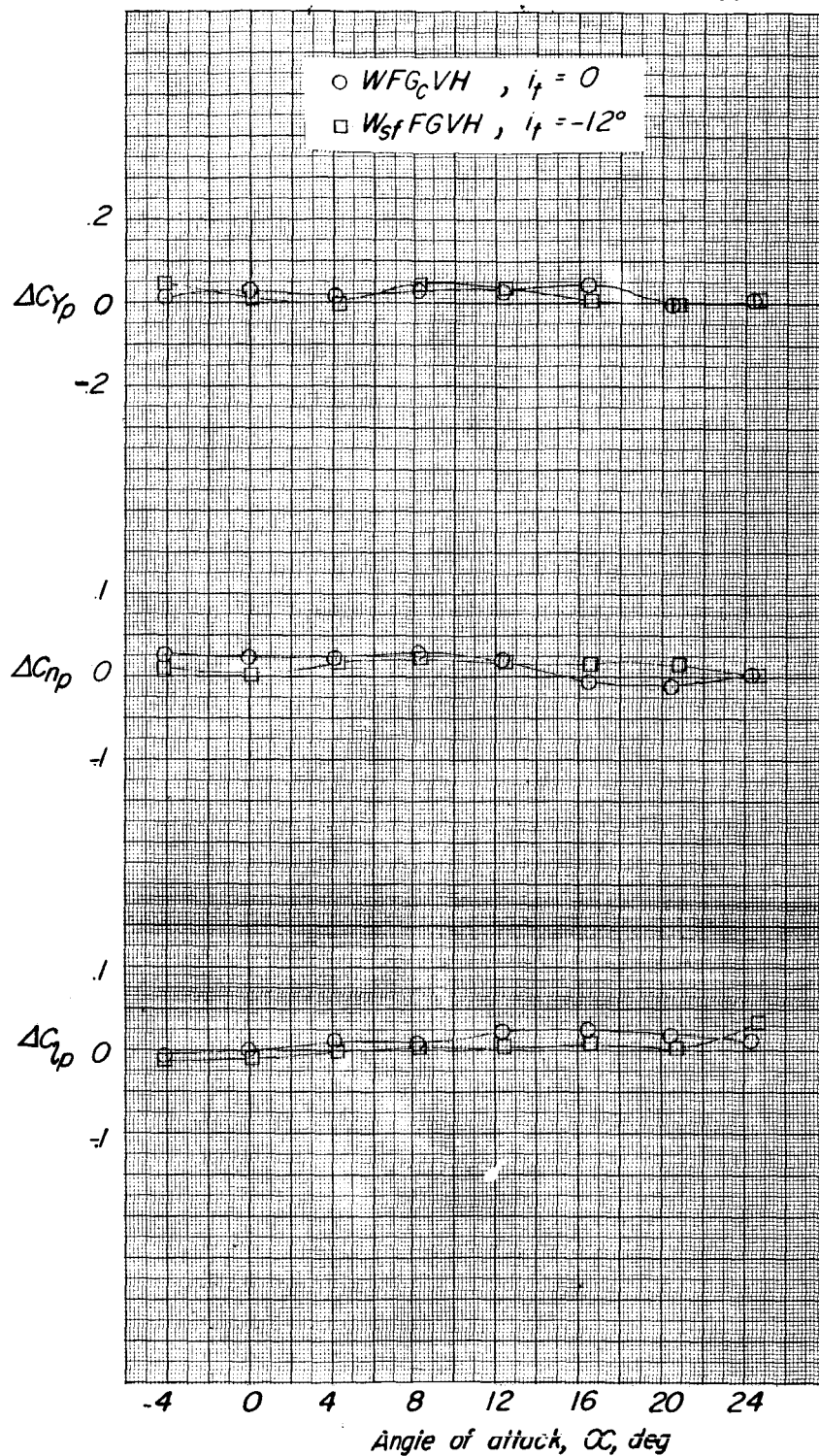


Figure 8.- Support-strut tare increments ΔC_{yp} , ΔC_{np} , and ΔC_{lp} plotted against angle of attack for the WFG_cVH configuration and a complete landing configuration.